
This item was submitted to [Loughborough's Research Repository](#) by the author.
Items in Figshare are protected by copyright, with all rights reserved, unless otherwise indicated.

Filtration and sedimentation behaviour of fibre/particle binary suspensions

PLEASE CITE THE PUBLISHED VERSION

PUBLISHER

Filtration Society

VERSION

AM (Accepted Manuscript)

LICENCE

CC BY-NC-ND 4.0

REPOSITORY RECORD

Chellappah, Kuhan, E.S. Tarleton, and Richard J. Wakeman. 2009. "Filtration and Sedimentation Behaviour of Fibre/particle Binary Suspensions". figshare. <https://hdl.handle.net/2134/5414>.

This item was submitted to Loughborough's Institutional Repository (<https://dspace.lboro.ac.uk/>) by the author and is made available under the following Creative Commons Licence conditions.



CC creative commons
COMMONS DEED

Attribution-NonCommercial-NoDerivs 2.5

You are free:

- to copy, distribute, display, and perform the work

Under the following conditions:

 **Attribution.** You must attribute the work in the manner specified by the author or licensor.

 **Noncommercial.** You may not use this work for commercial purposes.

 **No Derivative Works.** You may not alter, transform, or build upon this work.

- For any reuse or distribution, you must make clear to others the license terms of this work.
- Any of these conditions can be waived if you get permission from the copyright holder.

Your fair use and other rights are in no way affected by the above.

This is a human-readable summary of the [Legal Code \(the full license\)](#).

[Disclaimer](#) 

For the full text of this licence, please go to:
<http://creativecommons.org/licenses/by-nc-nd/2.5/>

FILTRATION AND SEDIMENTATION BEHAVIOUR OF FIBRE/PARTICLE BINARY SUSPENSIONS

K. Chellappah¹, E.S. Tarleton¹ (e.s.tarleton@lboro.ac.uk) and R.J. Wakeman^{1,2}

¹Advanced Separations Technology Group, Department of Chemical Engineering, Loughborough University, Loughborough, Leics., LE11 3TU, UK.

²Consultant Chemical Engineer, Exeter, EX5 1DD, UK.

ABSTRACT

The constant pressure filtration characteristics of cellulose fibres, titanium dioxide (rutile) and mixtures of the two were studied using a well controlled filtration apparatus. To interpret the filtration results, relevant fibre and particle physical properties were determined and the sedimentation behaviour of the binary suspensions quantified. The porosities (ϵ_{av}) of filter cakes formed from pure fibre and rutile suspensions were approximately 0.75 and 0.6 respectively. The general concept of additive porosity for binary mixtures agreed reasonably well with the experimental data. With filtrations at 450 kPa, the average specific cake resistances (α_{av}) for pure fibre and rutile in deionised water were approximately 9.4×10^{13} and 4.2×10^{12} m kg⁻¹ respectively, with the variation of α_{av} with fibre fraction showing a minimum. Similar trends were observed at filtration pressures of 150 and 600 kPa. No minimum in α_{av} was observed with 450 kPa filtrations of suspensions made using 0.1 M CaCl₂ solution. It is concluded that the influences of solids composition and solution environment on α_{av} are substantial for fibre/particle mixtures whilst the influence of filtration pressure is less evident.

INTRODUCTION

Fibrous solids are known to induce complexities in filtration due to their irregular shapes, high aspect ratios and wide size distributions. A significant proportion of process/waste streams that require dewatering contain fibrous or similarly elongated solids, and are usually complex mixtures containing various solids of differing sizes, shapes and surface properties. Examples of industries where such suspensions may be commonplace include water and wastewater treatment, paper and pulp, and pharmaceutical (where needle shaped particles are often encountered). The study of binary suspensions containing particles and fibres are therefore of significant industrial and academic interest as such systems are representative of process/waste streams involving one solids component, which can be colloidal in nature, and another which is much larger and of a high aspect ratio. Despite its importance, there appears to be a sparsity of research on the cake filtration of fibrous suspensions, and particularly for binary suspensions containing particles and fibres.

The properties of a filter cake at any given time during filtration depend, to a large extent, on the packing behaviour of its constituent particles. The packing behaviour increases in complexity when there is more than one solids phase and/or a range of particle sizes and shapes. Typical theoretical predictions for spherical binary mixtures show a minimum porosity at some intermediate mixture fraction (generally attributed to interparticle penetration)¹⁻⁵. Theoretical¹⁻⁵ and experimental³⁻⁷ works suggest that the larger the difference in size between the coarse and fine particles in a mixture so the more pronounced is the non-linearity in the porosity versus solids composition relationship. Most pertinent to the deadend filtration of binary suspensions are the works of Shirato *et al.*⁸, Abe and Hirose⁹, Wakeman¹⁰ and Iritani *et al.*¹¹.

Besides size and shape, physico-chemical properties can play an important role in particle packing during cake formation. For instance, electrostatic interactions between particles and the effect of solution environment on filtration performance has been highlighted and studied by several workers in the past¹¹⁻¹³. After lamenting that the effects of physico-chemical factors on filtration

performance have received little or no attention for binary suspensions, Iritani *et al.*¹¹ discussed the influence of electrostatic interactions on the filtration of titania (rutile) and silica mixtures. They found that under the conditions where titania-silica aggregation occurred, the trend of specific cake resistance with solids composition showed a shallow minimum. No such shallow minimum was evident in the absence of titania-silica aggregation.

This paper discusses the filtration performance of fibrous as well as binary (fibre and titania (rutile)) suspensions. The influence of suspension composition, filtration pressure and solution environment on filtration is discussed in relation to cake properties such as average cake porosity (ϵ_{av}) and average specific cake resistance (α_{av}). Discussions are aided by the analysis of sedimentation behaviour for identical suspensions.

EXPERIMENTAL

Apparatus and Methods

A computer controlled, laboratory scale, pressure filtration apparatus capable of automated data acquisition was used for the filtration experiments. Briefly, the hardware comprised a stainless steel (s/s) deadend Nutsche filter of 120 cm² area and a s/s suspension storage vessel connected by s/s piping and computer controlled electro-pneumatic valving. The filtration pressure was maintained at a constant level via an electronically driven regulator whilst filtrate flow was determined via successive readings from an electronic balance. Positioned within the filter cell were 10 titanium micro-pressure transducers attached to custom made s/s holders and micro-bore tubes. These were used in an attempt to determine liquid pressure profiles within a filter cake during filtration; although the response and accuracy of the transducers were proven in validation experiments with calcium carbonate (calcite) and pure rutile, the majority of pressure profiles could not be captured reliably due to the significant voidage inherent in filter cakes containing fibres. Further details of the apparatus can be found elsewhere^{14,15}. The filter medium was a Gelman Versapor 0.2 μm rated membrane. A new membrane was used in each experiment and this yielded a visually clear filtrate in all cases. Sedimentation experiments were carried out in a plastic graduated cylinder of 360 mm length and 59.5 mm inner diameter. The suspension-supernatant interface height and corresponding elapsed time were recorded at suitable intervals.

Suspensions consisting of either pure fibres, or rutile, or binary mixtures of the two, in deionised water or 0.1 M CaCl₂ solutions were used. In both filtration and sedimentation experiments the feed solids concentration was maintained at 1.1% v/v. In experiments involving CaCl₂, a 0.1 M solution was prepared prior to any solids addition. In an experiment involving a binary mixture, rutile was added into the suspending medium and mixed for 30 minutes at 600 rpm prior to fibre addition in order to reduce dispersion problems. The final suspension was stirred for approximately 3 h at 800 rpm with a flat blade stirrer prior to filtration or sedimentation. Care was taken to ensure that suspensions were well mixed to minimise batch to batch variations. Experiments were carried out at a constant temperature of 21 \pm 2°C and over a narrow pH range. The pH of suspensions in deionised water ranged from approximately 8.4 (pure rutile) to 7.6 (pure fibres) and in 0.1 M CaCl₂ solution from 6.9 (pure rutile) to 7.3 (pure fibres).

Materials and Characterisation

The fibres used were in the form of tissue paper (Merton Cleaning Supplies, Leicester). When the tissue paper was dispersed into deionised water two types of suspended solids were produced, cellulose fibres and the fillers associated with the tissue. Energy dispersive X-ray spectroscopy (EDX) determined calcite to be the filler and acid washing coupled with mass balances determined that approximately 4.8% v/v of the tissue paper comprised of these calcite fillers. The titania was in the form of the rutile polymorph and obtained from Huntsman. The true density of the fibres (including fillers) and rutile were 1300 kg m⁻³ and 4200 kg m⁻³, respectively. Typical Scanning

Electron Micrograph (SEM) images of the rutile and fibres are shown in Figure 1.

Rutile particle size distributions and zeta (ζ) potentials in deionised water were measured with a Malvern Zetasizer 3000 HS. Due to the high aspect ratio and non-uniform shape of the fibres, neither light scattering nor photon correlation spectroscopy could be used for reliable fibre size distribution measurements. The size (width) distributions of the fibres were therefore obtained by measuring more than a hundred fibres at various magnifications of SEM image. Figure 2 shows the cumulative size distributions by number for rutile and fibres.

The SEM images in Figure 1 show that rutile is elliptical in shape and slightly elongated with an aspect ratio of 2-4. The fibres are generally non-cylindrical with aspect ratios expected to be more than 10, and more likely in the region of 100; although determinations were difficult, estimates were obtained by examining images of individual fibres 'rubbed-off' from samples of the tissue paper. From Figure 2 it is evident that the median particle size for rutile and median width of fibres were 0.45 μm and 15 μm respectively, with the fibres displaying a much wider size distribution. The standard deviation of fibre widths was 10.8 μm .

The ζ -potential of the rutile and fibres in deionised water and 0.1 M CaCl_2 at varying pH values were calculated from measured electrophoretic mobilities using the Smoluchowski equation and the results are presented in Figure 3. There were no limitations in using the Zetasizer for measuring fibre ζ -potential as the Smoluchowski equation can be applied to particles of arbitrary shape provided the particle dimensions are much greater than the electrical double layer thickness¹⁶. For suspensions in deionised water, the ζ -potential values were approximately -18 mV for fibres and -35 mV for rutile over the experimental pH range of interest. For suspensions in 0.1 M CaCl_2 solution, ζ -potential values were approximately -5 mV for fibres and +21 mV for rutile where Ca^{2+} ions appear to adsorb onto the fibre and rutile surfaces.

RESULTS AND DISCUSSION

All filtration experiments were performed at constant pressure and analysed to establish values of average specific cake resistance (α_{av}) and cake porosity (ϵ_{av}) using:

$$\frac{dt}{dV} = \frac{\mu\alpha_{av}\rho_l s}{A^2\Delta P(1-ms)}V + \frac{\mu R_m}{A\Delta P} \quad (1)$$

$$\epsilon_{av} = 1 - \frac{w}{\rho_s \left(\frac{V s (\rho_s (m-1) + \rho_l)}{A \rho_s (1-ms)} \right)} \quad (2)$$

where V is the filtrate volume, t the filtration time, A the filtration area, ΔP the constant filtration pressure, μ the filtrate dynamic viscosity, ρ_l the liquid density, ρ_s the solids density, s the solids mass fraction in the feed, m the ratio of mass of wet cake to the mass of dry cake as measured at the end of filtration, R_m the membrane resistance and w the mass of dry solids deposited per unit filter area. α_{av} was determined in the conventional manner from the initial linear portion of dt/dV vs. V plots. Initial settling rate in a sedimentation test was determined from a plot of suspension-supernatant interface height vs. time, where the initial points fall on a straight line whose gradient can be calculated. The proportion of sludge is the final sediment height (after 24 h settling) expressed as a percentage of the initial suspension height.

The experimental data presented are representative of the dataset obtained during the investigation. Error bars shown for some datasets indicate the level of reproducibility. The effects of solids composition on binary suspension filtration are presented in terms of the variable X_D

which is defined as the ratio of the volume of fibres to the total volume of solids in the suspension; $X_D = 0$ indicates a pure rutile suspension (i.e. no fibres) whereas $X_D = 1$ indicates a pure fibre suspension (i.e. no rutile).

General Behaviour of Single Component Suspensions

Filtrations of suspensions containing fibres were carried out at various pressures between 50 and 600 kPa. Figure 4 shows a typical plot of cumulative filtrate volume vs. time at a pressure of 450 kPa; data for the filtration of a rutile suspension at the same pressure is included for comparison. Rutile, and particularly fibre, suspensions in deionised water were generally difficult to filter and formed cakes of relatively high resistance. Filtration of fibre suspensions at various pressures and with other filter media (a 4 μm rated filter cloth was also trialled) were unexpectedly slow. Compressibility index values (n value in the well known relationship $\alpha_{av} = \alpha_0(1-n)\Delta P^n$) were determined to be approximately 0.7 for pure fibre cakes and 0.1 for pure rutile cakes. These values indicate moderate compressibility and near incompressible behaviour, respectively.

Pure rutile settled faster in 0.1 M CaCl_2 solution than in deionised water due to suppression of the electrical double layer which promoted aggregation (the initial settling rate in CaCl_2 solution and deionised water were $3.2 \times 10^{-2} \text{ m s}^{-1}$ and $1.1 \times 10^{-5} \text{ m s}^{-1}$ respectively). Pure fibre suspensions did not readily settle in either solution environment as the constituent fibres appeared to be networked in the settling cylinder. Pure fibre suspensions of lower total solids concentrations settled more readily and the initial settling rate was greater in 0.1 M CaCl_2 solution. By way of example, at a solids concentration of 0.16% v/v, the fibre initial settling rate was 0.14 m s^{-1} in 0.1 M CaCl_2 solution and 0.039 m s^{-1} in deionised water.

General Behaviour of Binary Suspensions

Figure 5 shows batch sedimentation results for suspensions of various solids compositions in deionised water and 0.1 M CaCl_2 solution. The results are presented in the form of initial settling rates and proportion of sludge vs. X_D to assist in: (1) qualitative assessments of the degree of physico-chemical interactions (state of aggregation); (2) determination of packing characteristics at different solids compositions and solution environments; and (3) estimates of the degree of sedimentation which is likely to occur during a filtration.

It is seen from Figure 5 that pure rutile and pure fibre in deionised water appear to be stable suspensions which do not readily settle. With only small amounts of fibres added to a pure rutile suspension, rutile-fibre interactions take place and the suspension de-stabilises. The initial settling rate continues to increase with X_D up to the point where ~50% by volume of the solids consists of rutile, presumably due to the increasing surface area available for interaction. Further increases in X_D caused a sharp reduction in initial settling rate until approximately 75% by volume of the solids consisted of fibres, and subsequent increases in X_D rendered the suspension essentially stable once again. It is interesting that $X_D = 0.5$ is also the approximate region where the proportion of sludge begins to undergo a more marked increase. The general sedimentation trends for suspensions in deionised water and CaCl_2 solution appear to be similar. Initial settling rates in the range $0.1 < X_D < 0.8$ were lower for suspensions in CaCl_2 solution, presumably due to the formation of low density, loosely networked aggregates. The presence of more loosely networked aggregates in CaCl_2 solution was evidenced by the greater proportions of sludge at a given X_D .

Examples of dt/dV vs. V plots for 450 kPa filtrations of binary suspensions in deionised water and CaCl_2 solution are shown in Figures 6 and 7, respectively. It is seen that a greater variation in filtration behaviour is observed with the suspensions in deionised water; note the different scales on the y-axes. An interesting observation from Figures 6 and 7 is the presence of abrupt changes in the filtrate flow rate part way through some filtrations. Such transitions have been noted by previous workers¹⁷⁻²⁰ and attributed to the migration of fines, cake collapse and/or formation of channels within the cake. These abrupt transitions are currently the subject of further investigation.

Figures 8 and 9 show the effects of solids composition and filtration pressure on ε_{av} and α_{av} for filtrations at 150, 450 and 600 kPa. Figures 10 and 11 show the effects of solids composition and solution environment on ε_{av} and α_{av} for 450 kPa filtrations from deionised water and 0.1 M CaCl₂. Error bars for some data are included to illustrate the level of reproducibility. The behaviour shown in Figures 8-11 is described and interpreted in the following sections.

Effects of Solids Composition

Typical theoretical predictions for spherical binary mixtures show a minimum in the variation of porosity with solids composition whereby a larger difference in size between the coarse and fine particles generally yields a more pronounced non-linearity. However, in this study, the variation of porosity with volume fraction of fibres is shown to be relatively limited and in many cases almost linear despite the fibres being of wide size distribution and generally several orders of magnitude larger than the rutile particles. By way of example, two models are presented and compared to illustrate the fibre/rutile packing characteristics. The first attempts to describe the concept of interparticle penetration (Tokumitsu model²¹) and the second the concept of additive porosity (Shirato additive law⁸).

The following two equations have been proposed by Tokumitsu²¹ to predict the porosity of a packed bed formed from a binary mixture of particles. For a packed bed rich in small particles: and for a packed bed rich in large particles:

$$\varepsilon_{av} = 1 - \frac{1 - \varepsilon_2}{(1 - X_D) + X_D \left(1 + 1.4 \left(\frac{x_2}{x_1} \right) \right) (1 - \varepsilon_2)} \quad (3)$$

$$\varepsilon_{av} = 1 - \frac{1 - \varepsilon_1}{X_D \left(1 + \left(\frac{x_2}{x_1} \right)^{\frac{1}{3}} \left(\left(1 + \frac{1 - X_D}{X_D} \right)^{\frac{1}{3}} - 1 \right) \right)^3} \quad (4)$$

where x_1 is the size of large particles (fibres in this case) and x_2 the size of small particles (rutile in this case). Correspondingly, ε_1 and ε_2 are the average porosities of pure fibre and rutile filter cakes, respectively. Briefly, equation (3) attempts to describe penetration of large particles into a packed bed of fines and equation (4) attempts to describe penetration of fines into a packed bed of large particles. Further details of the physical meaning behind equations (3) and (4) are discussed by Abe and Hirose⁹. Predictions of ε_{av} given by equations (3) and (4) for cakes formed at 450 kPa are plotted in Figure 8 along with the experimental data to illustrate a typical theoretical prediction assuming interparticle penetration. Similar trends were obtained using equations (3) and (4) on the 150 and 600 kPa data. Similar trends were also obtained when an 'equivalent packing diameter', x_{p1} , was used instead of x_1 (fibre width) in equations (3) and (4). The equivalent packing diameter of a non-spherical solid is defined by Yu and Standish^{22,23} as the diameter of a sphere having the same size-dependent packing behaviour as the solid and can be expressed for fibrous solids as:

$$X_{p1} = \left(3.1781 - 3.6821 \frac{1}{\psi} + 1.5040 \frac{1}{\psi^2} \right) \left(1.145 \left(\frac{L}{x_1} \right)^{\frac{1}{3}} x_1 \right) \quad (5)$$

where ψ is the fibre sphericity and L the fibre length. Moreover, Yu and Standish^{22,23} claim that the equivalent packing diameter is a useful concept in relating non-spherical packing to spherical packing.

Using the Shirato additive law⁸, the additive porosity is given by the sum of the void volumes divided by the sum of the total volumes due to each component:

$$\varepsilon_{av} = \frac{\frac{\varepsilon_1 X_D}{1 - \varepsilon_1} + \frac{\varepsilon_2 (1 - X_D)}{1 - \varepsilon_2}}{\frac{X_D}{1 - \varepsilon_1} + \frac{1 - X_D}{1 - \varepsilon_2}} \quad (6)$$

Predictions of ε_{av} given by the Shirato additive law are plotted in Figure 8 along with the experimental data. It is immediately seen that equation (6) represents the data better than equations (3) and (4) and assuming the theoretical justifications of both models hold, this brings about some physical implications. As discussed by Heertjes and Zuideveld²⁴, a drawback of the Shirato additive law is that the filling of a pore volume generated by one component by another (finer) component cannot be described. Considering the fibre and rutile shapes and the size distributions, the fibres may be coated by rutile to reduce the interfibre porosity to a small extent. However, Figure 8 suggests that the general concept of additive porosity seems to be better than interparticle penetrations when one particle is adsorbed onto the surfaces of the other.

The trend of α_{av} with solids composition for filtrations from deionised water passes through a minimum in the region $0.3 < X_D < 0.7$ (Figure 9). This minimum is an interesting result as in many cases specific resistance has previously been reported to decrease gradually and become lowest when $X_D = 1$ ^{8,10}. However, a similar minimum in α_{av} at an intermediate X_D value was recently reported by Iritani *et al.*¹¹ when aggregation occurred between the two solids phases (rutile and silica) of the binary mixtures filtered. Iritani *et al.* did not observe a minimum in α_{av} in the absence of such aggregation. Similarly, the most likely reason for the concave α_{av} vs. X_D trend observed in the present work is rutile-fibre aggregation. A contributing factor may be simultaneous sedimentation which leads to size classification within the cake; larger solids are more prevalent closer to the medium which promote a reduced α_{av} . The α_{av} vs. X_D trend for suspensions in deionised water corresponds to the trend of initial settling rate vs. X_D (Figure 5) where the greatest initial settling rates were obtained in the region $0.3 < X_D < 0.6$. This comparability is not surprising as the initial settling rates were largely influenced by the degree of aggregation. Furthermore, the influence of simultaneous sedimentation is most significant for suspensions which give the greatest initial settling rates. However, a more explicit relationship between α_{av} and initial settling rate cannot be easily formulated because: (1) at higher fibre concentrations suspensions tend to become structured, thereby altering the settling behaviour; (2) settling rates will be reduced for loosely networked aggregates (lower effective density difference between the settling solids and suspending liquid); and (3) complications arise from simultaneous sedimentation during filtration.

An increase in fibre volume fraction (X_D) results in fractionally more porous cakes (larger ε_{av}) and also in a greater mean 'size'. Hence, increasing values of X_D may be expected to result in more permeable filter cakes (i.e. lower α_{av}). However, when fibres dominate the filtration further complexity is introduced by a fibre's ability to coil up and to mat out. Yet more complications arise due to the presence of solids of widely varying shapes and sizes in the fibrous suspension with fines potentially being present which leads to conditions conducive to blinding.

Effects of Filtration Pressure

The porosities of all binary mixture cakes were slightly greater at 150 kPa than at 450 and 600 kPa, presumably because the aggregates were able to maintain a more open structure at the lower pressure. However, in general, the effects of filtration pressure on ε_{av} seem to be limited. Furthermore, the effects of filtration pressure on α_{av} are less evident relative to the effects of solids composition and solution environment. One noticeable effect is the increase in α_{av} for filtrations of $0.3 < X_D < 0.7$ suspensions at the highest pressure of 600 kPa, which is not surprising as the

extent of aggregation is seemingly greatest over this solids composition range and so the filter cake compressibility may be expected to be relatively high. A direct consequence of the increase in α_{av} is that the minimum observed in the α_{av} vs. X_D trend for filtrations at 600 kPa became less pronounced.

Effects of Solution Environment

With filtrations at 450 kPa, α_{av} values for rutile ($X_D < 0.3$) and fibre ($X_D > 0.7$) rich cakes were significantly lower for the suspensions in 0.1 M CaCl_2 solution (Figure 11). The reduction in α_{av} for feeds of pure rutile in CaCl_2 solution corresponded with increases in cake porosity and initial settling rate. The reduction in α_{av} for rutile rich cakes was therefore attributed to suppression of the rutile electrical double layer resulting in a larger effective particle size. The reduction in α_{av} for fibre rich cakes was more significant and more difficult to reconcile. A 0.1 M CaCl_2 solution environment reduced α_{av} values for pure fibre cakes by two orders of magnitude. Potential reasons include charge, packing and/or swelling effects.

Swelling of the fibres in CaCl_2 solution will result in a larger fibre size and hence lower α_{av} . Although swelling may be a contributing factor, parameter proportionality shows that to solely account for the reduction in α_{av} the effective fibre width will have to increase by more than ten times its original width in deionised water which seems unlikely. Changes to fibre packing in the presence of CaCl_2 may alter the volume specific surface in contact with the fluid (S_v). To solely account for the reduction in α_{av} , S_v would need to decrease by approximately fifteen times its original value in deionised water. Due to the high aspect ratio of the fibres, such a reduction in S_v may be plausible via changes to fibre orientation. Although charge effects on fibres may initially appear to be insignificant due to their large size, it is perhaps the most likely reason for the reduction in α_{av} . The fines present in the fibre suspensions may have been removed (aggregated) in the presence of CaCl_2 . The fines, along with wide shape and size distributions, may be responsible for the large α_{av} value with feeds of pure fibre in deionised water in the first place. The fines aggregation hypothesis is further supported by the fact that: 1) at a lower concentration (0.16% v/v), the initial settling rate for pure fibres was greater in 0.1 M CaCl_2 solution than in deionised water; 2) the supernatant of a settled fibre suspension in deionised water was significantly more turbid than the supernatant of a corresponding suspension in 0.1 M CaCl_2 solution; and (3) the fibrous solids were close to their iso-electric point in 0.1 M CaCl_2 .

Taking into account that the fibres and rutile were oppositely charged in CaCl_2 solution, the effect of CaCl_2 solution environment on rutile-fibre interactions could be expected to be greater than on rutile-rutile and fibre-fibre interactions as rutile-fibre electrostatic repulsions were not just reduced but altered to become attractive forces. However, there was little variation in ϵ_{av} (Figure 10) and α_{av} (Figure 11) due to CaCl_2 addition in the solids composition range $0.3 < X_D < 0.7$. This apparent discrepancy may be explained by the fact that α_{av} cannot be expected to continually decrease and ϵ_{av} to continually increase with increased states of aggregation as there will eventually be a lower limit to the packing fraction under a given applied pressure. This limit seems to have already been reached by cakes formed from suspensions in deionised water over the solids composition range $0.3 < X_D < 0.7$.

CONCLUSIONS

Filtration data presented in this paper indicate the significance of physico-chemical interactions as the most likely cause of minima in the trend of α_{av} with solids composition for feeds in deionised water. The influence of solids composition was most pronounced in the absence of CaCl_2 and the influence of solution environment was most pronounced at the extremes of solids composition (i.e. rutile rich and fibre rich). For rutile rich cakes, the reduction in α_{av} due to CaCl_2 addition was most likely via suppression of the rutile electrical double layer. For fibre rich cakes, although several hypotheses have been postulated, definitive reasons for the reduction in α_{av} due to CaCl_2 addition

were not apparent. Compared to the influence of solids composition and solution environment, the influence of filtration pressure on α_{av} was less significant. The general concept of additive porosity seems to be better than interparticle penetration when one particle is adsorbed onto the surfaces of the other.

NOMENCLATURE

A	filtration area (m^2)
m	ratio of mass of wet cake to dry cake (-)
n	compressibility index (-)
ΔP	filtration pressure (Pa)
R_m	filter medium resistance (m^{-1})
S_v	specific surface (m^{-1})
s	mass fraction of solids in suspension (-)
t	cake formation time (s)
V	cumulative filtrate volume (m^3)
w	mass of dry solids deposited per unit area ($kg\ m^{-2}$)
X_D	ratio of volume of fibres to the total volume of solids in a binary suspension (-)
x	particle size (width for fibres) (μm)
α_{av}	average specific resistance of a filter cake ($m\ kg^{-1}$)
α_0	average specific resistance at unit applied pressure ($m\ kg^{-1}\ Pa^{-n}$)
μ	liquid viscosity (Pa s)
ε_{av}	average filter cake porosity (-)
ρ_L	liquid density ($kg\ m^{-3}$)
ρ_S	true density of solids or effective solids density for binary mixtures ($kg\ m^{-3}$)

Subscripts

1	Referring to fibres
2	Referring to rutile

REFERENCES

1. Yu A.B., Zou R.P. and Standish N., 1996, Modifying the linear packing model for predicting the porosity of non-spherical particle mixtures, *Industrial Engineering Chemistry Research*, **35**, 3730-3741.
2. Yu A.B. and Standish N., 1988, An analytical-parametric theory of the random packing of particles, *Powder Technology*, **55**, 171-186.
3. Mota M., Teixeira J.A., Bowen W.R. and Yelshin A., 2001, Binary spherical particle mixed beds: Porosity and permeability relationship measurement, *Trans. Filtration Society*, **1**(4), 101-106.
4. Dias R., Teixeira J.A., Mota M. and Yelshin A., 2004, Particulate binary mixtures: Dependence of packing porosity on particle size ratio, *Industrial Engineering Chemistry Research*, **43**, 7912-7919.
5. Leclerc D., 1975, Characteristics of unconsolidated filter media in *The Scientific Basis of Filtration*, Ives K.J. (Ed.), pp.151-166, Nato Advanced Study Institute Series, Noordhoff, Leyden.

6. McGeary R.K., 1961, Mechanical packing of spherical particles, *J. American Ceramic Society*, **44**, 513-522.
7. Suzuki M., Yagi A., Watanabe T. and Oshima T., 1986, Estimation of the void fraction in a bed randomly packed with particles of three sizes, *International Chemical Engineering*, **26**, 491-498.
8. Shirato M., Sambuichi M. and Okamura S., 1963, Filtration behavior of a mixture of two slurries, *American Institute Chemical Engineers J.*, **9**, 599-605.
9. Abe E. and Hirose H., 1982, Porosity estimation of a mixed cake in body filtration, *J. Chemical Engineering Japan*, **13**, 490-493.
10. Wakeman R.J., 1996, Characteristics of filtration using solids added to the suspension as a body aid, *Proc. 7th World Filtration Congress*, pp.234-238, Hungarian Chemical Society, Budapest.
11. Iritani E., Mukai Y. and Toyoda Y., 2002, Properties of a filter cake formed in dead-end microfiltration of binary particulate mixtures, *J. Chemical Engineering Japan*, **35**, 226-233.
12. Wakeman R.J., Sabri M.N. and Tarleton E.S., 1991, Factors affecting the formation and properties of wet compacts, *Powder Technology*, **65**, 283-292.
13. Koenders M.A. and Wakeman R.J., 1997, Filter cake formation from structured suspensions, *Trans. Institution Chemical Engineers*, **75**, 309-320.
14. Tarleton E.S. and Hadley R.C., 2003, The application of mechatronic principles in pressure filtration and its impact on filter simulation, *Filtration*, **3**(1), 40-47.
15. Tarleton E.S., 2008, Cake filter scale-up, simulation and data acquisition – A new approach *J. Chinese Institute Chemical Engineers*, **39**, 151-160.
16. Hunter R.J., 2001, *Foundations of Colloid Science*, 2nd Edn., Oxford University Press, Oxford.
17. Rietema K., 1953, Stabilising effects in compressible filter cakes, *Chemical Engineering Science*, **2**, 88-94.
18. Fathi-Najafi M. and Theliander H., 1995, Determination of local filtration properties at constant pressure, *Separation Technology*, **5**, 165-178.
19. Sørensen P.B., Christensen J.R. and Bruus J.H., 1995, Effect of small scale solids migration in filter cakes during filtration of waste water solids suspensions, *Water Environmental Research*, **67**, 25-32.
20. Tarleton E.S. and Morgan S.A., 2001, An experimental study of abrupt changes in cake structure during dead-end pressure filtration, *Trans. Filtration Society*, **1**(4), 93-100.
21. Tokumitsu Y., 1964, On the packing of granular materials, *J. Material Science Japan*, **13**, 752-758.
22. Yu A.B. and Standish N., 1993, Characterisation of non-spherical particles from their packing behaviour, *Powder Technology*, **74**, 205-213.
23. Ai-Bing Yu, Nicholas Standish and Arnold McLean, 1993, Porosity calculation of binary mixtures of nonspherical particles, *J. American Ceramic Society*, **76**, 2813-2816.

24. Heertjes P.M. and Zuideveld P.L., 1978, Clarification of liquids using filter aids, Part III: Cake resistance in surface filtration, *Powder Technology*, **19**, 45-64.

FIGURES AND TABLES

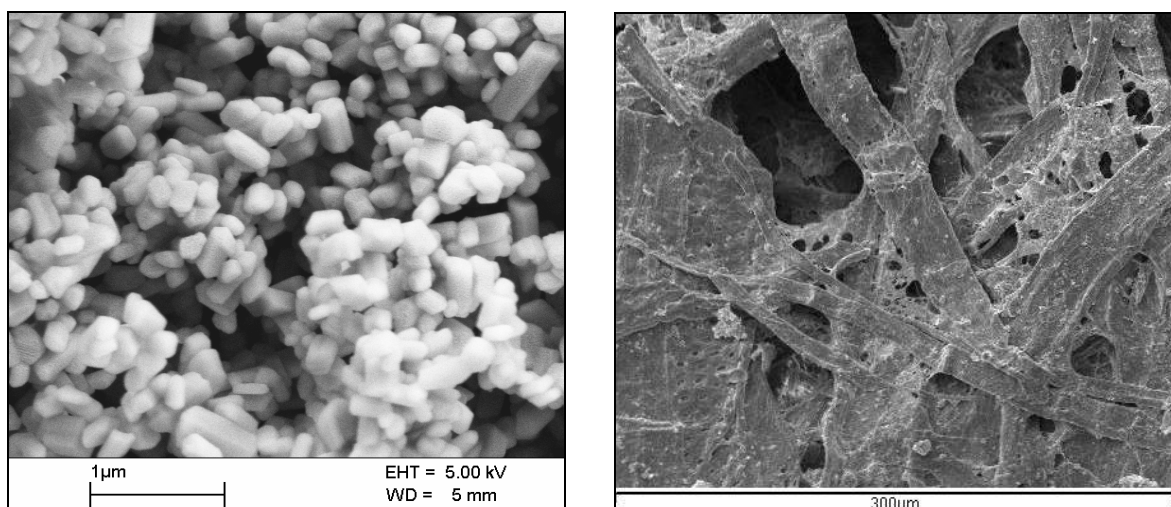


Figure 1: SEM images of the rutile (*left*) and fibres with associated calcite fillers (*right*).

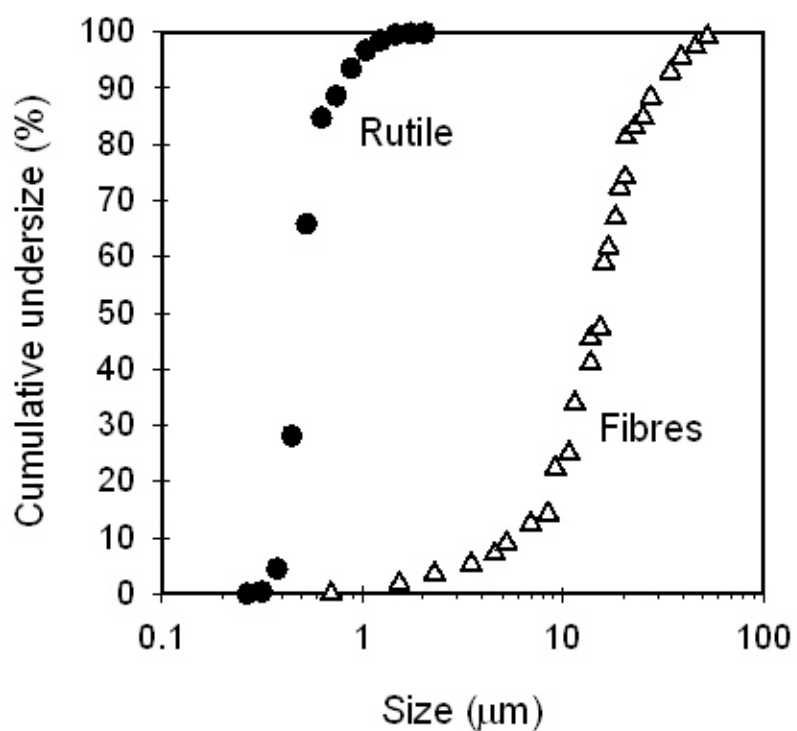


Figure 2: Cumulative size (width for fibres) distributions of the fibres and rutile in deionised water.

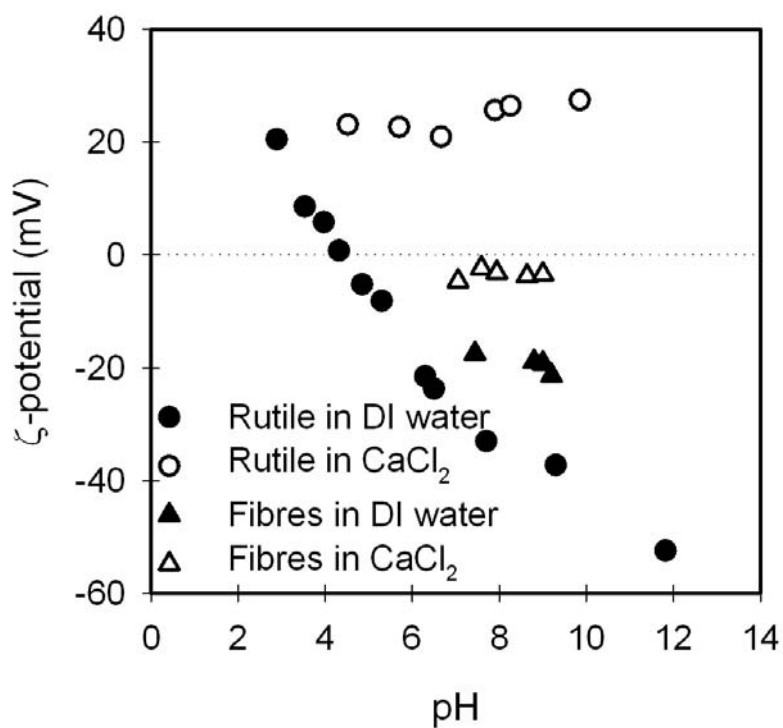


Figure 3: Zeta potential variation with pH for rutile and fibres in deionised water and 0.1 M CaCl₂.

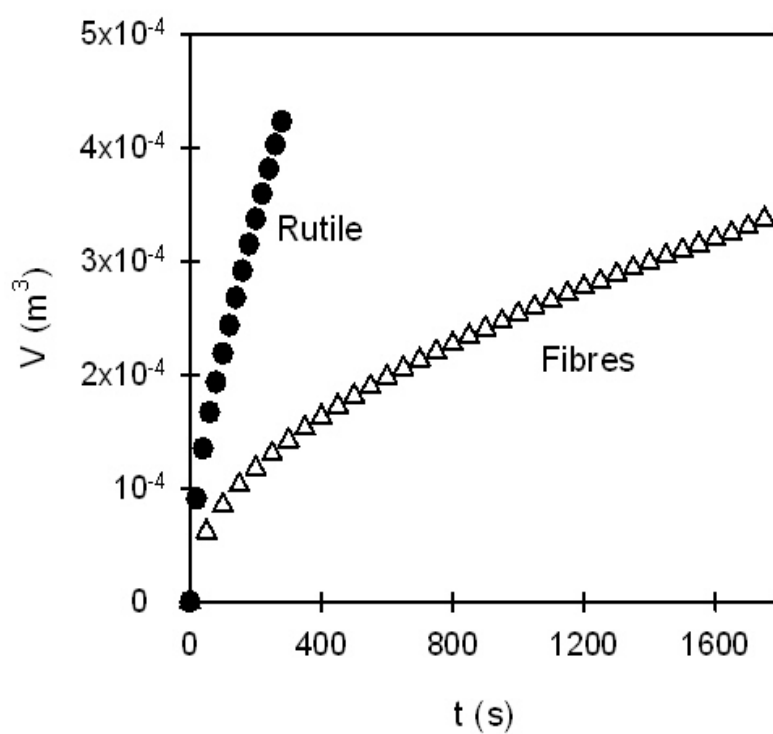


Figure 4: Plots of cumulative filtrate volume versus time for filtrations of 1.1% v/v fibre and rutile suspensions in deionised water at a constant pressure of 450 kPa.

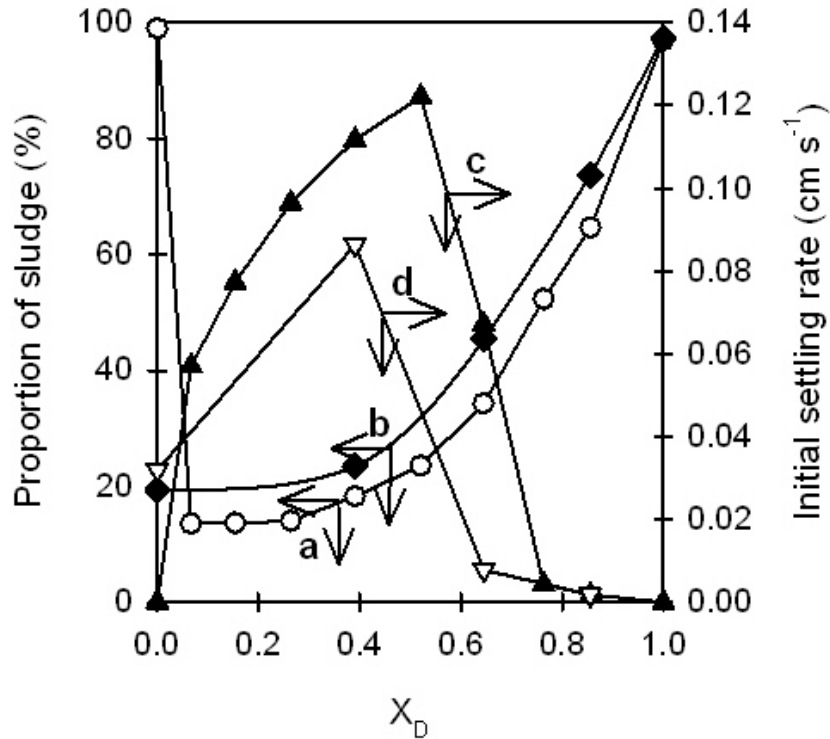


Figure 5: Effects of fibre fraction (X_D) on the proportion of sludge and initial settling rate (a = proportion of sludge in deionised water; b = proportion of sludge in 0.1 M CaCl₂ solution; c = initial settling rate in deionised water; d = initial settling rate in 0.1 M CaCl₂ solution).

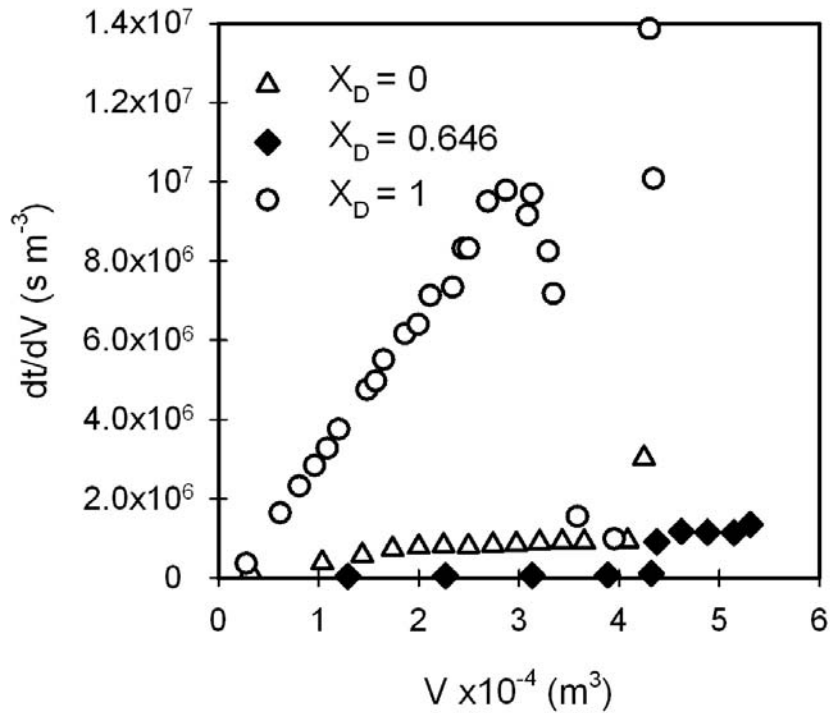


Figure 6: Examples of dt/dV vs. V plots for the filtration of binary suspensions in deionised water at a constant pressure of 450 kPa.

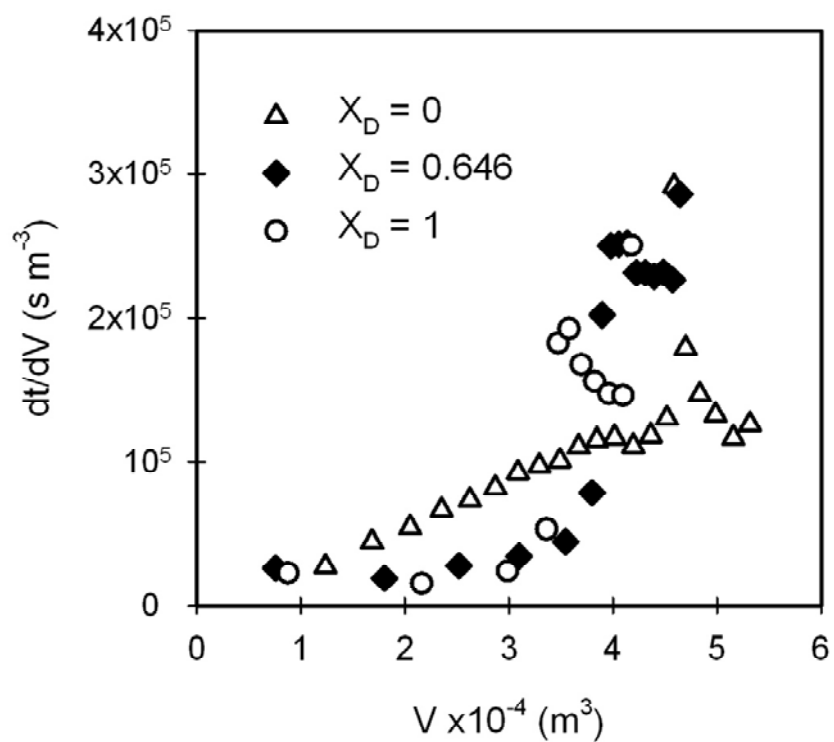


Figure 7: Examples of dt/dV vs. V plots for the filtration of binary suspensions in 0.1 M CaCl_2 solution at a constant pressure of 450 kPa.

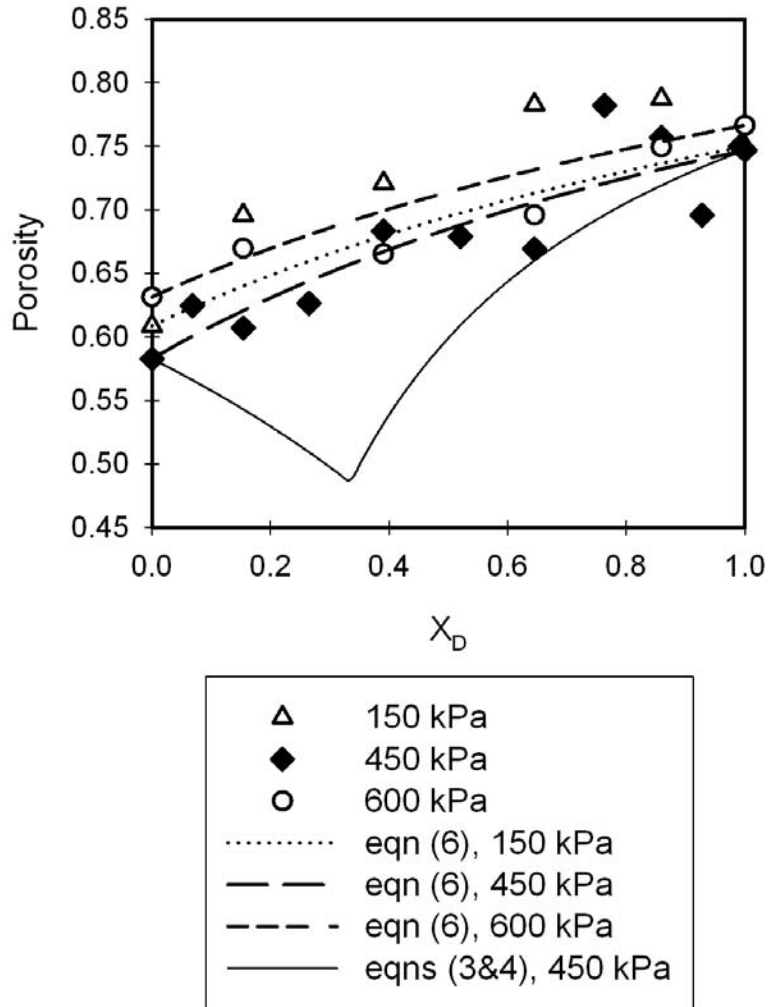


Figure 8: Effects of solids composition on ϵ_{av} for filtrations from deionised water at constant pressures of 150, 450 and 600 kPa. The prediction given by equations (3) and (4) is included for the 450 kPa data and predictions given by equation (6) are included for all pressures.

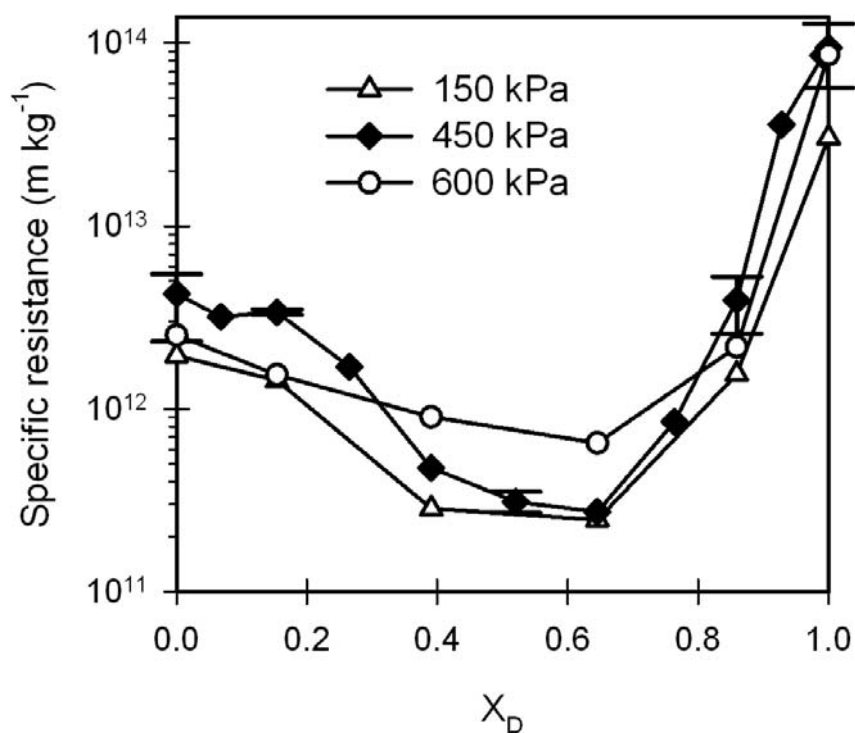


Figure 9: Effects of solids composition on α_{av} for filtrations from deionised water at constant pressures of 150, 450 and 600 kPa.

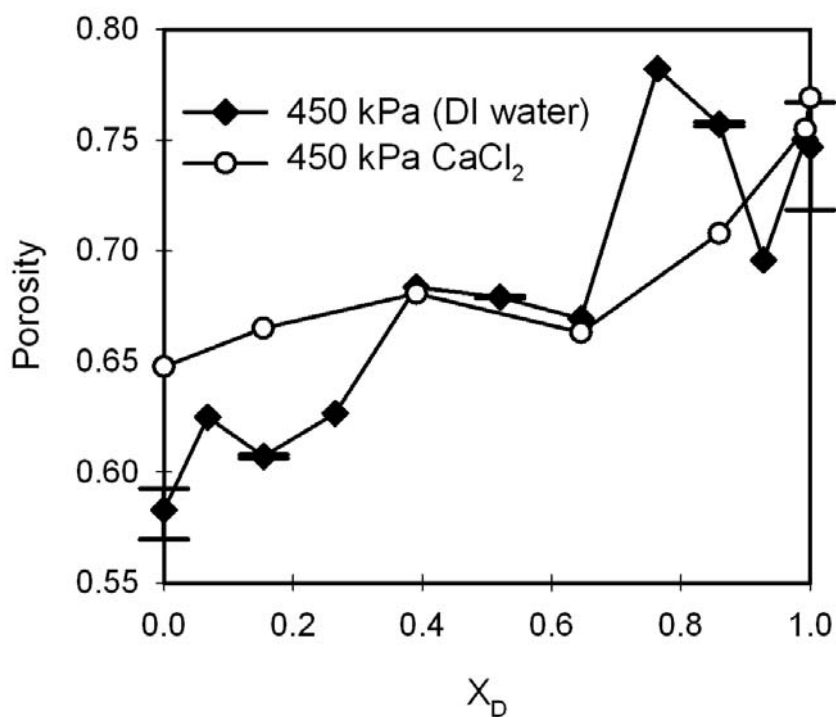


Figure 10: Effects of solids composition on ε_{av} for 450 kPa filtrations from deionised water and 0.1 M CaCl₂.

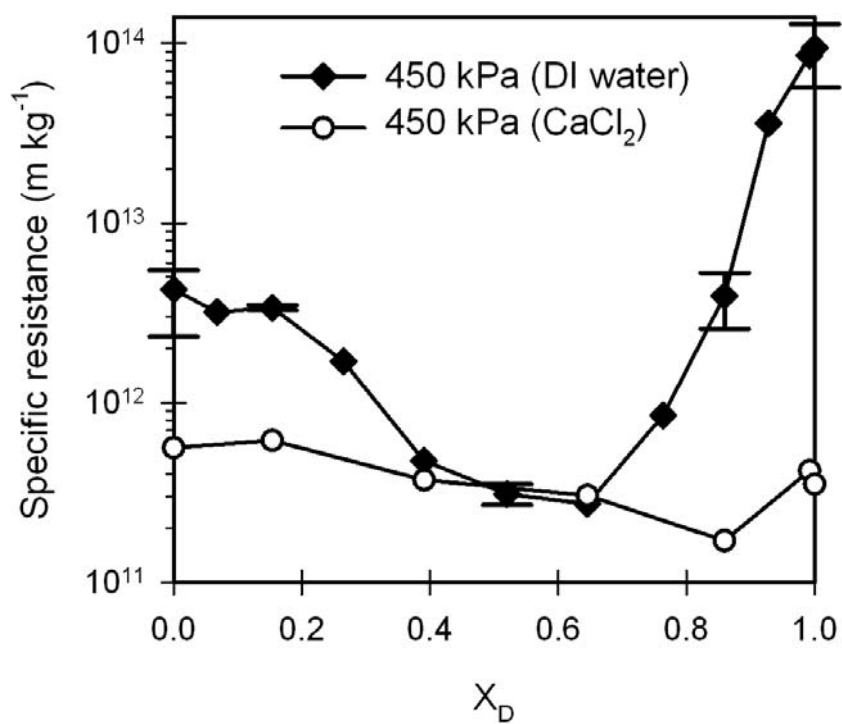


Figure 11: Effects of solids composition on α_{av} for 450 kPa filtrations from deionised water and 0.1 M CaCl₂.